Quantifying knapping actions: a method for measuring the angle of blow on flakes

Li Li[1] · Jonathan S. Reeves[2] · Sam C. Lin[3,4] · Claudio Tennie[1,5] · Shannon P. McPherron[5]

Abstract

Stone artifacts are critical for investigating the evolution of hominin behavior—they are among our only proxies for hominin behavior in deep time. Hominin cognition and skill are often inferred by reconstructing the technical decisions hominins made throughout the knapping process. However, despite many advancements in understanding how hominins knapped, some of the key factors involved in past flake production cannot be easily/readily derived from stone artifacts. In particular, the angle at which the knapper strikes the hammer against the core to remove the flake, or the angle of blow, is a key component of the knapping process that has up to now remained unmeasurable on archeological assemblages. In this study, we introduce a new method for estimating the angle of blow from the ventral surface of flakes. This method was derived from a controlled experiment that explicitly connects fracture mechanics to flake variability. We find that a feature of the flake's bulb of percussion, what we call the bulb angle, is a measurable indicator of the angle of blow. Our experimental finding is further validated in two additional datasets from controlled and replicative knapping experiments. These results demonstrate the utility of continuing to link flake variation with technical decision-making to fracture mechanics. In addition, they also provide a useful and relatively simple means to capture a currently invisible aspect of hominin stone tool production behavior.

Keywords Knapping actions · Experimental archeology · Fracture mechanics · Bulb angle · Angle of blow

✉ Li Li
li.li@uni-tuebingen.de

1   Department of Early Prehistory and Quaternary Ecology, Eberhard Karls University of Tübingen, Hölderlinstraße 12, 72074 Tübingen, Germany

2   Technological Primates Research Group, Max Planck Institute for Evolutionary Anthropology, Deutscher Platz 6, 04103 Leipzig, Germany

3   Centre for Archaeological Science, School of Earth, Atmospheric and Life Sciences, University of Wollongong, Northfields Ave, Wollongong, NSW 2522, Australia

4   Australian Research Council Centre of Excellence for Australian Biodiversity and Heritage, University of Wollongong, Northfields Ave, Wollongong, NSW 2522, Australia

5   Department of Human Evolution, Max Planck Institute for Evolutionary Anthropology, Deutscher Platz 6, 04103 Leipzig, Germany

Introduction

Much of what is known about the evolution of hominin cognition and behavior is derived from the study of stone tools. Today, researchers routinely employ a wide array of analytical approaches to reconstruct the technical decisions and processes underlying hominin knapping strategies in the past (Pelegrin 1993; Boëda 1995; Texier and Roche 1995; Roche et al. 1999; Delagnes and Roche 2005). Knapping is without a doubt a complex motor process that involves interactions of different body parts (Susman 1998; Biryukova and Bril 2008; Bril et al. 2010; Geribàs et al. 2010; Nonaka et al. 2010; Williams et al. 2012; Rein et al. 2013), and archeologists have come to recognize the importance of understanding this dynamic process by combining methods such as replicative experiments, refitting, and other technological approaches (Eren et al. 2016). A key aspect of these technological approaches is in underlining the importance of manual gestures and knapping actions in lithic reduction (Forestier 1992; Pelegrin 1993; Texier and Roche 1995; Roche et al. 1999). Knappers need to flexibly apply different manual gestures along the knapping sequence to

effectively navigate the changing interactions among different functional parameters, including configurations of the striking platform and various force application variables like the hammer striking speed and angle (Roussel et al. 2009; Geribàs et al. 2010; Rein et al. 2013; Vernooij et al. 2015; Baena et al. 2017; Cueva-Temprana et al. 2019). Some studies of modern knappers suggest that these gestural skills and "know-hows" may be acquired through learning and practice, highlighting the significance of cultural transmission in hominin stone tool making (Lycett 2013; Morgan et al. 2015; Lycett et al. 2016; Pargeter et al. 2019). There are also studies that suggest that the technical "know-how" required for making early stone tools can be acquired via individual learning (Tennie et al. 2016, 2017; Snyder et al. in press). Moreover, because knapping actions ultimately depend on the biomechanics of the human musculoskeletal structure, increasingly researchers have focused on examining the relationship between stone percussive activities and hominin skeletal morphologies (Rolian et al. 2011; Marzke 2013; Macchi et al. 2021).

One component of knapping gestures that has been repeatedly observed to be critical in controlling the flaking process is the angle at which the hammer strikes the core, or the angle of blow (e.g., Hellweg 1984, Fig. 1). It has been said that striking a hammer perpendicularly straight into the core runs the risk of crushing the platform and generating step fractures and incipient cones, while increasing the angle of blow by tilting the platform and swinging the hammer in an arc helps facilitate flake detachment (Whittaker 1994: 95). Importantly, variation in the angle of blow has been shown to be one of the main parameters that separate novice from expert knappers (Vernooij et al. 2015). For instance, experimental studies carried out by Geribàs et al. (2010) and Cueva-Temprana et al. (2019) both showed that novices tend to prefer striking the hammer in a more direct angle of blow, while experts can effectively control different striking angles to achieve a desired result (Geribàs et al. 2010; Rein et al. 2013; Cueva-Temprana et al. 2019). The importance of controlling the angle of blow also varies with the knapping strategy and goals. For instance, the ability to apply appropriate angles of blow has been shown to be critical in biface production, especially during biface thinning (Shipton 2018).

Varying the angle of blow also appears to affect various characteristics of a detached flake such as its linear dimensions, bulb of percussion, and the presence of platform lipping. The controlled flaking experiment by Speth (1972, 1975) described that flakes made with larger angles of blow are generally shorter and have a less prominent bulb of percussion than those produced under a more direct hammer strike (Soriano et al. 2007). Several studies have also shown that in addition to producing a less prominent bulb
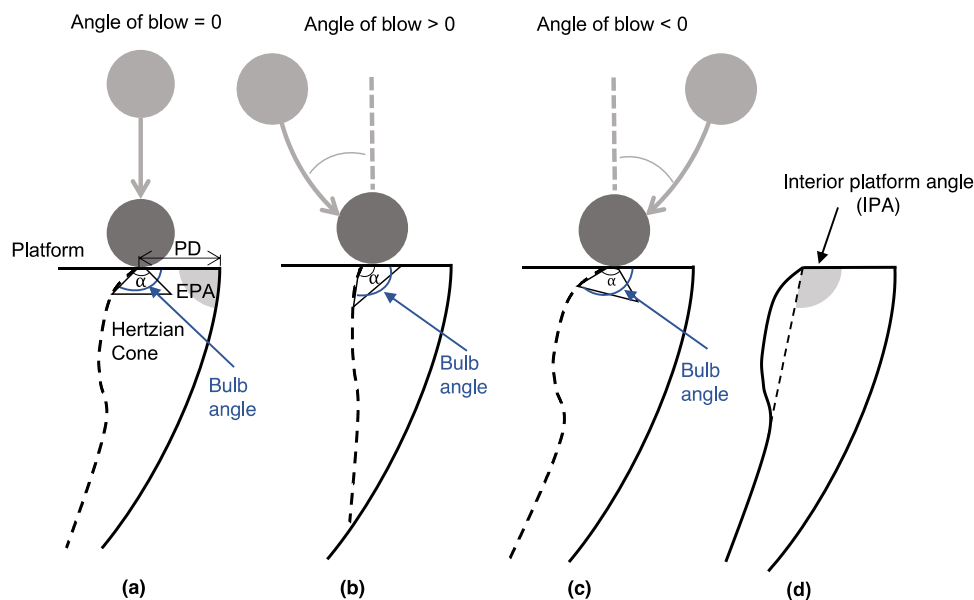

Fig. 1 Schematic illustration of bulb angle and its comparison with interior platform angle on a flake from its profile view. The Hertzian cone generated from the hammer blow is represented by the triangle beneath the hammer, and α refers to the Hertzian cone angle, which is approximately 136 degrees in soda-lime glass. The bulb angle is the angle between the flake's platform and the extruding side of its Hertzian cone, as is marked in dark blue. (a) Showing that the Hertzian cone's central line remains perpendicular to the platform when angle of blow is zero, the bulb angle should be 158 degrees. Platform depth (PD) and exterior platform angle (EPA) are also shown in the figure; (b) showing the case when the Hertzian cone is completely pushed to the platform, the bulb angle should equal the Hertzian cone angle; (c) showing the case when the Hertzian cone is tilted into the core, the theoretical bulb angle should be greater than 158 degrees; (d) showing interior platform angle as defined in Dibble and Whittaker (1981)

of percussion, a more oblique hammer strike may increase the chance of platform lipping (Bataille and Conard 2018; Schmid et al. 2019, 2021). Speth argued that this might be due to the limited stress exerted on the platform by the higher angles of blow. Similarly, Hellweg (1984) noted that increasing the striking angle during knapping would lead to the detachment of shorter flakes. In a later experiment using a similar controlled flaking setup to that of Speth's (1972), Dibble and Whittaker (1981) found no obvious impact from the angle of blow on flake dimensions, though the authors suggested that the negative outcome may be related to confounding variables in the experimental design. More recently, using a more developed mechanical flaking apparatus, Dibble and Rezek (2009) showed that flakes produced from higher angles of blow are indeed smaller in mass. The same pattern was reported by Magnani et al. (2014), who found that flake linear dimensions such as length and width, relative to platform depth, decreased as the angle of blow increased. In other words, two identically prepared cores struck in identical locations with identical hammers will produce two different flakes depending on the angle of blow.

Despite its known effect on various flake attributes, there has been no direct way of measuring the angle of blow from the lithic artifacts themselves. Crabtree (1972) suggested that the angle of blow could be reconstructed by the interior platform angle of the detached flake, yet Dibble and Whittaker (1981) showed that this is not the case in their controlled experiment. More recently, Magnani et al. (2014) described the angle of blow as archeologically invisible and suggested that any inference about the angle of blow will have to be derived from its effect on flake attributes such as bulb size and flake shape. However, these attributes are also under the influence of other independent knapping factors, and so reconstructing the angle of blow from these attributes will be difficult. As a consequence, the angle of blow is routinely left out of archeological applications of flake attribute analysis and, to a certain extent, general flake formation models. For instance, in a series of controlled experiments, Dibble and colleagues tested for and recognized the influence of the angle of blow on flake attributes (Dibble and Rezek 2009), yet they inevitably focused on the effects of exterior platform angle (EPA) and platform depth (PD), both of which are directly observable on flakes, to summarize flake size and shape (Dibble and Whittaker 1981; Dibble and Pelcin 1995; Dibble and Rezek 2009; Rezek et al. 2011; Magnani et al. 2014; Leader et al. 2017; Dogandžić et al. 2020). While the EPA-PD model of flake formation, where flake mass is modeled as a function of the combined effect of exterior platform angle and platform depth, has been proven valid in both experimental and archeological assemblages (Lin et al. 2013; Režek et al. 2018; Braun et al. 2019; Dogandžić et al. 2020), it remains unclear how the angle of blow fits into this model. To begin tackling this question, it

is necessary to first address the challenge of measuring the angle of blow directly from stone flakes.

In this study, we turned to fracture mechanics and the basic principles of brittle solid fracture to study the visible traces that the angle of blow produces on the detached flake. In the fracture mechanics literature, it has been repeatedly shown that an oblique hammer blow (i.e., a non-zero angle of blow) will *tilt* the Hertzian cone so that its central line is no longer perpendicular to the platform (Lawn et al. 1984; Chaudhri and Chen 1989; Salman et al. 1995; Suh et al. 2006; Chaudhri 2015). Modern knappers have also noted the possible relationship between the angle of blow and the angle of the Hertzian cone (Hellweg 1984; Whittaker 1994; Waldorf 2006). As shown in Fig. 1, the Hertzian cone is tilted relative to the platform surface when the hammer strike is not perpendicular to the platform. Because the Hertzian cone initiates the formation of the bulb of percussion, it should be possible to detect the change in the Hertzian cone's orientation, brought on by varying hammer strike angles, in the initial angle of the bulb of percussion on a flake's interior surface. Specifically, this angle, which we refer to hereafter as the bulb angle, is measured immediately at the intersection between a flake's platform and the protruding side of the Hertzian cone before it bends back to form the bulb of percussion (Fig. 1, Fig. 2). Defined this way, a bulb angle of 90 degrees indicates a flat interior surface of the flake with no visible bulb of percussion. As this angle increases from 90 degrees, the Hertzian cone becomes more apparent, and the bulb becomes more prominent. Note
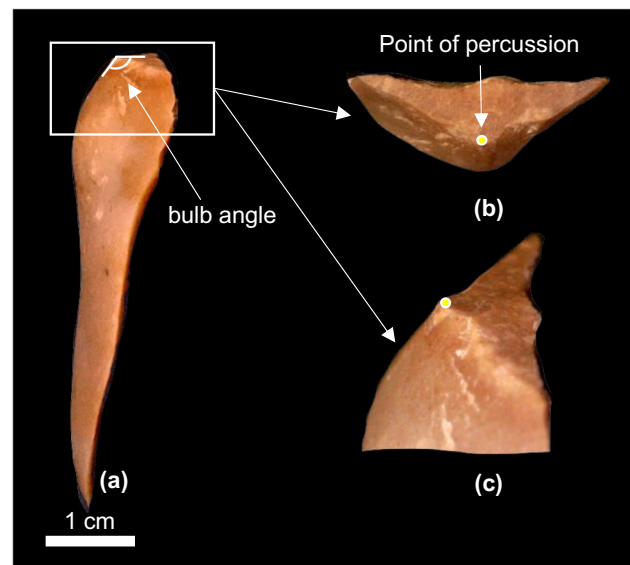

Fig. 2 Bulb angle identified on a flint flake from this study. (a) Showing the zoom-out view of bulb angle on the profile side of the flake with a 1-cm scale bar; (b) and (c) showing zoomed-in views of the flake's platform and partial bulb of percussion. The point of percussion is marked by the white dot

that the bulb angle is different from the interior platform angle, which has been defined as the angle between the platform and the flake's ventral surface *without* considering the curvature of the bulb of percussion (Dibble and Whittaker 1981, Fig. 1d).

Key here is that Hertzian cone angles are constants within each raw material type. In the case of soda-lime glass, it has been shown experimentally that the Hertzian cone angle is approximately 136 degrees (Roesler 1956; Lawn et al. 1974; Kocer and Collins 1998). That means, when the central line of the Hertzian cone is perpendicular to the platform, the angle between either edge of the cone and the platform is 22 degrees (180 degrees in a flat platform, minus a 136-degree cone, divided by the two sides the cone intersects a plane). Theoretically then, a flake detached with a zero angle of blow from a soda-lime glass core should have a bulb angle of 158 degrees (i.e., 136 degrees from the Hertzian cone plus 22 degrees between the inner edge of the cone and the platform surface; see Fig. 1a). Based on observations made in previous fracture mechanics studies (Lawn et al. 1984; Chaudhri and Chen 1989; Salman et al. 1995; Suh et al. 2006; Chaudhri 2015), we hypothesize that as the angle of blow increases, the Hertzian cone will pivot outward towards the core's flaking surface, causing the bulb angle to decrease. Take the hypothetical scenario illustrated in Fig. 1b as an example, here the greater angle of blow causes the Hertzian cone to pivot into the flake to the point that the inner edge of the cone becomes aligned with the platform surface. In this scenario, we would expect the flake to exhibit a bulb angle that equals the Hertzian cone angle (i.e., 136 degrees). If, on the other hand, the hammer strike is into the core (i.e., negative angles of blow, Fig. 1c), the Hertzian cone will tilt away from the flake and into the core instead. In this case, we should see a more prominent blub of percussion and a bulb angle that is greater than 158 degrees.

Material and methods

Experimental design

To test our hypothesis of the relationship between bulb angle and angle of blow, we first conducted a controlled experiment using a "drop tower" setup to systematically investigate the effect of angle of blow on bulb angle. This experiment is henceforth referred to as the *drop tower experiment*. Drop tower setups were used in controlled flaking experiments from the 1970s to the 1990s (Speth 1972, 1975; Dibble and Whittaker 1981; Dibble and Pelcin 1995). This type of setup is effective for controlling both the striking location and angle of blow for a flaking event. As shown in Fig. 3, the drop tower used in our experiment adopts the design from these previous studies. Additionally, a commercially

Fig. 3 The drop tower setup used in this study. The laser level is not shown in the photo

Hammer controlled by an electromagnetic switch

Glass core clamped in the vice
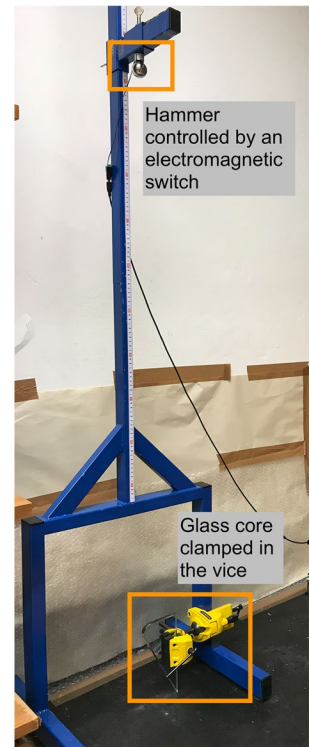
available self-leveling two-way (up and down) gravity-controlled laser (Huepar 621CR) was used to ensure precision of the strike location. A steel ball bearing with a diameter of 16 mm was used as the hammer. We were able to achieve a strike location precision of about 2 mm. This precision impacts mainly our ability to control the platform depth. For each set of angles of blow, we varied platform depth from around 7 ($\pm$ 2 mm) up to 20 mm ($\pm$ 2 mm). Plate (soda-lime) glass with a thickness of 10 mm was used as the core material. The plate glass was cut with a diamond blade wet saw to prepare an exterior platform angle of 65 degrees for all cores. A total of 103 flakes (henceforth the *drop tower dataset*) were made using the plate glass cores with angles of blow ranging from $-$ 20 to 60 degrees in 10-degree intervals. To control the angle of blow, glass cores were secured in a clamping vice which allowed for the relative position of the core platform to be altered (Fig. 3). In other words, in this type of setup, the angle of blow is altered by pivoting the core platform surface relative to a horizontal plane. We positioned a digital angle gauge on the flake platform to measure the angle between the flake platform and the horizontal, which is equal to the angle of blow. More information regarding the setup is provided in the Supporting Information. We measured the bulb angle (see below) and platform depth on each of the flakes coming from this experiment.

To verify the results from the drop tower experiment, we measured the bulb angle on 3D models of glass flakes produced with known angles of blow by Dibble and colleagues in previous controlled experiments (Dibble and Rezek 2009;

Rezek et al. 2011; Magnani et al. 2014; Leader et al. 2017; Dogandžić et al. 2020). This dataset is henceforth referred to as the *Dibble dataset*. Flakes from this dataset were selected to have no broken platforms, clear bulbs of percussion, and no platform lipping and were made with a steel hammer. These flakes were scanned and landmarked following protocols outlined in Archer et al. (2018). Low-quality scans, here defined as having a file size of less than 5 MB, were excluded because the detail of the platform was insufficient to make a reliable measurement of the bulb angle. In total, we obtained reliable data on 53 flakes from the Dibble collection with angles of blow of 0, 5, 10, 20, 30, and 40 degrees. These flakes were made on cores with exterior platform angles varying from 65 to 95 degrees with a 10-degree interval, though the majority of flakes have either a 65- or 75-degree exterior platform angle. Note that these angle of blow intervals in the Dibble dataset are different from that used in the drop tower experiment. More information regarding the 3D flake models is provided in the Supporting Information.

To test whether the bulb angle was sensitive to changes in the angle of blow in a less controlled setting, we conducted a blind test on a small set of flintknapped flakes produced at the Max Planck Institute for Evolutionary Anthropology. This dataset is henceforth referred to as the *MPI dataset*. To produce this dataset, two knappers (SPM and JR) each produced two sets of flakes using hard hammer percussion on two flint nodules from the Bergerac region of southwest France. Cobble hammerstones of varying sizes were used. The first set ($n = 16$) was made by the knappers consciously tilting the core to strike with the highest angle of blow that resulted in a flake removal. The second set ($n = 16$) was made with a deliberate effort to strike as directly or perpendicularly as possible into the platform (i.e., a zero angle of blow). In total, 64 flakes were produced between the two knappers, and each flake was given a random ID number along with the name of the knapper and the intended level of angle of blow as either "high" or "low." After excluding flakes with visible multiple Hertzian cones near the point of percussion, broken platforms, and broken bulbs near the point of percussion, 44 of the 64 flakes were selected for analysis. Of these 44 flakes, 14 were made from a nodule of black flint, and 30 flakes were made from a yellow flint nodule. Without prior knowledge of the associated knapper and angle of blow designation (high or low), one of us (LL) measured the bulb angle on the 44 flakes. These bulb angle values were merged with the MPI dataset using the random ID number once all of the flakes had been measured.

Measuring the bulb angle

For the flakes in the drop tower and MPI datasets, the bulb angle was measured with a manual goniometer with 1-degree precision as the angle between the platform surface and the extruding side of the Hertzian cone before it extends and integrates into the bulb of percussion. It should be noted that the measurement can be prone to measurement error due to the extremely small size of the Hertzian cone (the typical length of a Hertzian cone observed on the glass flakes in the drop tower dataset is about 1 to 2 mm), the platform curvature, and the overall curvature of the flake interior surface. While the Hertzian cone angle is mostly determined by the Poisson's ratio of the raw material (Roesler 1956; Frank and Lawn 1967; Kocer and Collins 1998), the size of the Hertzian cone is determined by a number of factors including the mechanical properties of both the hammer and the core, the size and shape of the hammer, and the applied force for flake removal (Fischer-Cripps 2007). It is also common for the Hertzian cone crack growth to alter its trajectory and forms a cone crack kink due to changes in the stress field as the crack propagates. This kinked growth inevitably increases the angle between the extended crack path and the contact surface (Kocer and Collins 1998; Fischer-Cripps 2007; Marimuthu et al. 2016). To avoid measuring bulb angle with the altered (kinked) Hertzian cone crack, we carefully position the joint of the goniometer at the point of percussion with one leg of the goniometer lying on the flake's platform surface and the other leg positioned against the extruding side of the Hertzian cone, at the very beginning of the flake's bulb of percussion (approximately 1 to 2 mm from the point of percussion, Fig. 4).

To further minimize measurement error and bias (Dibble and Rezek 2009), the bulb angle on each of the flakes in the drop tower dataset was measured on three separate occasions, and the bulb angle on each of the flakes in the MPI dataset was measured on four separate occasions (with no prior knowledge of the previous measurement results). The average of these measures was used in the final analysis. We also calculated the standard error (the standard deviation of bulb angle divided by the square root of the count of the total bulb angle measurements), standard deviation, and coefficient of variation of bulb angle for each flake in the two datasets. The bulb angle standard error captures the likely discrepancy between the actual average bulb angle calculated from the three measurements and the theoretical average bulb angle to be calculated from an infinite number of measurements. The standard deviation and coefficient of variation of bulb angle evaluate the variability of bulb angle for each flake. All three measurements help us estimate how accurately and reliably bulb angle is measured using a goniometer.

Two methods were used to measure the bulb angle from the 3D flake models in the Dibble dataset. The first method is referred to as the vector calculation method and uses scripts written in Python (Van Rossum and Drake 2011) and R (R Core Team 2020). In this method, first, we reorient each flake mesh

Fig. 4 Illustration of how the bulb angle is measured on a flake with a goniometer. (a) shows how the goniometer is placed on the flake to measure bulb angle, and (b) and (c) present a zoomed-in view of the bulb angle on a flake. Note that the 3D model of the flake used in the illustration is from the Dibble dataset, and it is for illustration purposes only
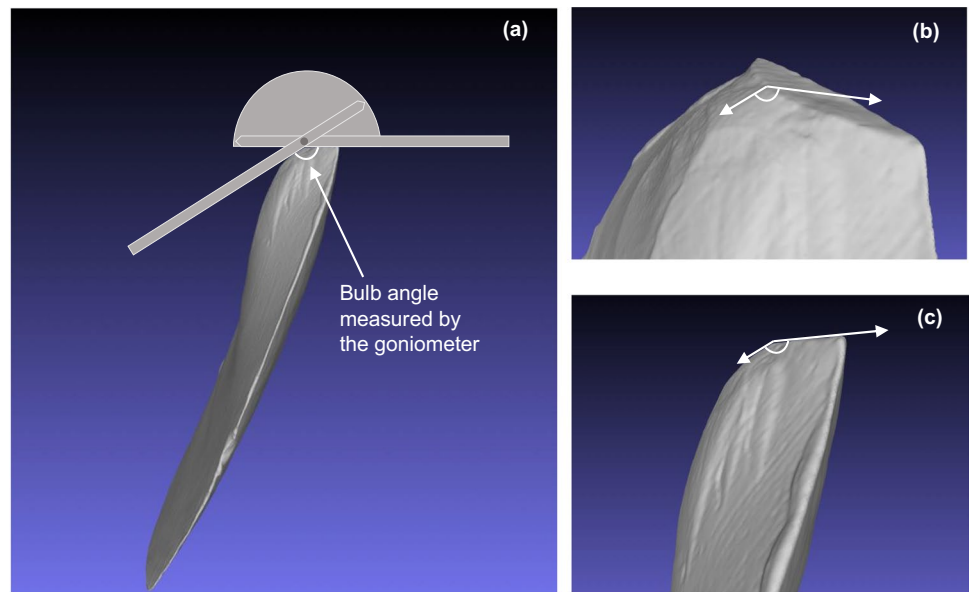
such that the point of percussion (P_0) is positioned at the origin point (0, 0, 0), the platform is coincident with the XY plane, the profile (longitudinal) section of the flake is perpendicular to the YZ plane, and the flake extends into negative Z space (Fig. 5a). Second, we extract the profile section (YZ) and intersect it with a circle centered at (0, 0) with a radius of 1, 2, or 3 mm. The points where the circle intersects the flake profile are labeled P_1 and P_2 (as marked in Fig. 5a). The bulb angle is then the angle between the vectors P_0P_1 and P_0P_2. The vector calculation method returns bulb angle with a precision of 0.01 degrees. The second method that we used for measuring

the bulb angle, which is referred to as the virtual goniometer method, uses the MeshLab (Cignoni et al. 2008) Virtual Goniometer Plugin developed by Yezzi-Woodley et al. (2021). To use the virtual goniometer, we first aligned the flake mesh following the above procedure described in step one of the vector calculation method. After that, we loaded the aligned flake mesh into MeshLab (Cignoni et al. 2008) and specified a patch centered at the flake's point of percussion using the Virtual Goniometer Plugin with a 1-, 2-, or 3-mm radius (Fig. 5b). As shown in Fig. 5b, the patch was then automatically divided by the platform edge of the flake: one half of the patch
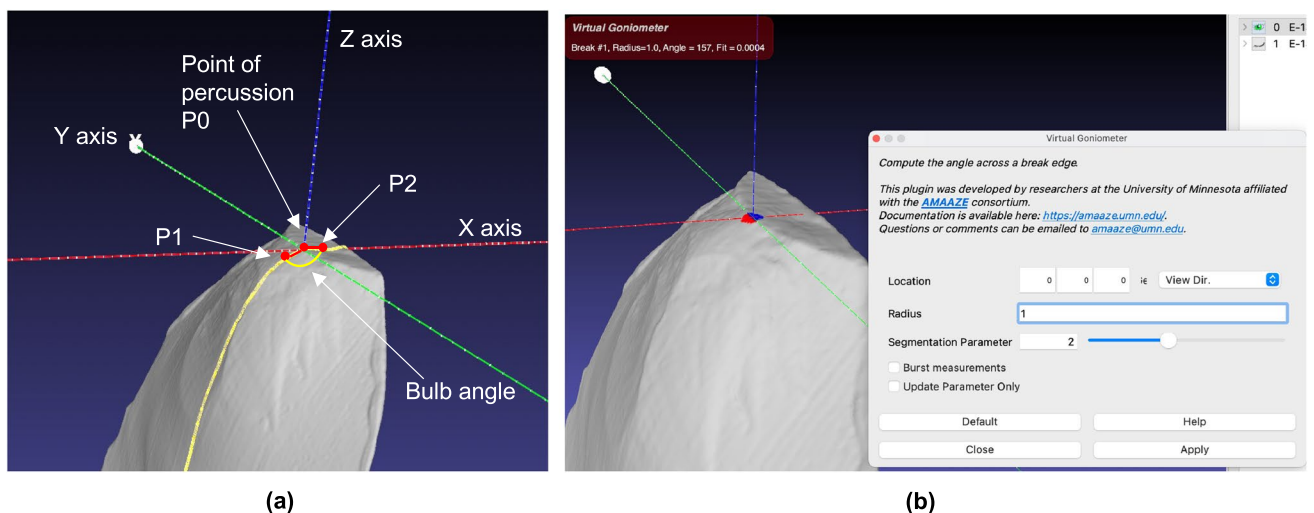
Fig. 5 Illustration of the two measurement methods on a 3D flake model from the Dibble dataset. (a) In the vector calculation method, bulb angle on the flake is defined as the angle between vectors P_0P_1 and P_0P_2. (b) In the virtual goniometer method with the Virtual Goni-ometer Plugin for MeshLab loaded (Yezzi-Woodley et al. 2021), bulb angle is defined as the angle between the red and blue patches marked on the flake model

on the flake's platform (colored in blue) and the other half on the flake's bulb of percussion (colored in red). The bulb angle was measured as the angle between these two sub-patches by the Virtual Goniometer Plugin with a precision of 1 degree.

As previously discussed, the Hertzian cone is a small-sized feature, and its crack can be susceptible to a kinked growth. In addition, the measurement of an angle on a 3D object is influenced by the location of the two end points that are chosen along the intersecting planes to form the angle from its vertex (Key et al. 2018; Valletta et al. 2020). It is thus important to determine the location of the end points of bulb angle from the point of percussion (the vertex of bulb angle). This helps ensure that bulb angle records the angle between the Hertzian cone crack and the platform surface before the cone crack kinks or extends to form the bulb of percussion to reflect the angle of blow to the greatest extent. To investigate the effect of end point location on bulb angle, we systematically compare the difference in bulb angle measured using the three intersection circle radii (1, 2, and 3 mm) for both 3D methods.

Statistical comparison

The experimental data were analyzed in three parts. First, for the Dibble dataset, we compared the difference in bulb angle measured with all three intersection circle radii for both 3D methods. Second, we considered the relationship between the measured bulb angle values and their associated hammer angle of blow across the three datasets. We used the Kruskal–Wallis test (also known as the one-way ANOVA on ranks), which assumes no particular distribution of the data, to examine whether there is a statistically significant difference in bulb angle between the angle of blow groups. Given our model and our sample sizes, our expectation was that there would be a noticeable, statistically significant difference in bulb angle between angle of blow groups wherein higher angles of blow produce lower bulb angles. Third, we use the linear regression model (ordinary least squares) to examine in addition to the angle of blow, whether changes in exterior platform angle and platform depth have a significant effect on bulb angle. For the drop tower dataset, only platform depth is included as an independent variable since exterior platform angle is a constant of 65 degrees. For the Dibble dataset, both exterior platform angle and platform depth are included as independent variables. Bulb angle is the response variable in both linear models. Given the fracture mechanics model, our expectation was that neither exterior platform angle nor platform depth has a significant effect on bulb angle. In all tests of statistical significance, we use a 0.05 level of probability for rejecting the null hypothesis.

We also apply linear regression to evaluate the usefulness of the bulb angle as an independent flake attribute for explaining variation in flake size, namely mass. Previous studies have shown that the mass of a flake can in part be explained by the exterior platform angle (EPA) and platform depth (PD). Based on this relationship, which is referred henceforth as the EPA-PD model, we construct three sets of linear regression models using the data obtained from the Dibble dataset. The first model is a baseline EPA-PD model that includes only EPA and PD as the independent variables, with flake mass as the response variable. The second model builds on the baseline model by including the known angle of blow as an additional predictor into the model. This model establishes the additional explanatory power of the angle of blow when accounting for variation in flake mass. Then, to evaluate how well the bulb angle acts as a proxy for the angle of blow, a third set of linear models are constructed by substituting the bulb angle measurements in place of the angle of blow as a predictor variable. Two separate models are constructed for the two different methods of measuring the bulb angle from the 3D flake models. Based on the three sets of models, we examine two questions. First, by comparing the first and second linear models, we examine whether the inclusion of the angle of blow helps improve the performance of the baseline EPA-PD model in predicting flake mass. Second, by comparing the second and third set of linear models, we assess if the bulb angle can serve as a reliable proxy measurement for the angle of blow.

For all linear models, the response variable, flake mass, was transformed to its cube root so that its dimensionality is comparable to the independent variables. As explained in Dibble and Rezek (2009), compared to the single-dimensional flake attribute platform depth, flake mass is a three-dimensional attribute similar to flake volume. It is thus important to bring these two variables to the same dimensionality for conducting analysis using linear models. Models were examined for their residual distribution, leverage, Cook's distance, and variance inflation factor. Model comparison was done using the ANOVA test. A significance level of 0.05 was used to assess whether the models with additional terms reduce the unexplained variability in flake mass. All other data analyses in this study are conducted in R (R Core Team 2020). All files needed to reproduce the results reported here and an explanation of the data are included in the Supporting Information and have been uploaded to Github (https://github.com/lili0824/bulb_angle).

Results

Evaluating the bulb angle measurement

For the drop tower dataset, the average standard error of bulb angle is 0.77 degrees (Fig. 4.1 in SI). That is, the overall possible discrepancy between the measured bulb angle and

the theoretical bulb angle is less than 1 degree. The overall standard deviation of bulb angle within each grouping of angle of blow is less than 3 degrees (Table 5.1 in SI 1). The overall coefficient of variation of bulb angle within each grouping of angle of blow is less than 25% (Table 5.1 in SI 1). For the Dibble dataset, the average bulb angle within each grouping of angle of blow systematically decreases as the intersection circle radius increases for both measuring methods (Fig. 4.2 and Table 5.3 in SI 1).

Drop tower dataset

For the drop tower dataset, there is a significant difference in bulb angle between the angle of blow groups (Fig. 6, Kruskal–Wallis test, $H = 84.709$, $p < 0.01$). The flakes produced with a zero angle of blow have an average bulb angle of 152.1 (± 1.91) degrees, which is not far off from the 158 degrees that we initially predicted based on Hertzian cone formation when the hammer strikes perpendicularly to the platform surface in soda-lime glass (Fig. 1a). As the angle of blow increases (i.e., the hammer strikes more obliquely), the bulb angle becomes smaller. As the angle of blow tilts to 40 degrees or more, the average bulb angle appears to stabilize at around 137 degrees. Again, this minimum bulb angle fits well with our predicted value of 136 degrees for when the Hertzian cone tilts to the point where one side of the cone is aligned with the platform surface (Fig. 1b). The regression model used to predict bulb angle with the angle of blow and platform depth can be found in SI 1. While the overall regression was statistically significant ($R^2 = 0.78$, F

$(2, 98) = 173.9$, $p < 0.001$), only the angle of blow accounts for variability in bulb angle ($p < 0.001$).

Dibble dataset

Here we will report the results of bulb angle measured with the 1-mm intersection circle for the two 3D methods. The same significant relationship between the angle of blow and the bulb angle as measured by both the vector calculation (Kruskal–Wallis test, $H = 25.037$, $p < 0.01$) and the virtual goniometer (Kruskal–Wallis test, $H = 24.698$, $p < 0.01$) methods is observed in the Dibble dataset (Fig. 7, see Table 5.2 in SI 1). Using the vector calculation method, the average bulb angle is 150.3 (± 5.4) degrees for flakes in the zero angle of blow group and is 135.3 (± 6.1) degrees for flakes in the 40-degree angle of blow group. Using the virtual goniometer method, the average bulb angle is 152.8 (± 4.7) degrees for flakes in the zero angle of blow group and is 134.3 (± 8.4) degrees for flakes in the 40-degree angle of blow group. Overall, the vector calculation method tends to return a smaller average bulb angle value than the virtual goniometer method (Fig. 8, see also Table 5.2 in SI 1). It should be noted that the standard deviation of bulb angle in the Dibble dataset is bigger than that in the drop tower dataset (Table 5.1 and Table 5.2 in SI 1). Unlike with the drop tower dataset, the maximum angle of blow represented in the Dibble dataset is 40 degrees. As such, we were not able to examine if the bulb angle reaches a plateau once the angle of blow tilts beyond 40 degrees.

The regression models used to predict bulb angle calculated using both the vector calculation and the virtual goniometer methods can be found in SI 1. For the vector

Fig. 6 Boxplot showing that bulb angle decreases as angle of blow (AOB) increases for flakes in the drop tower dataset
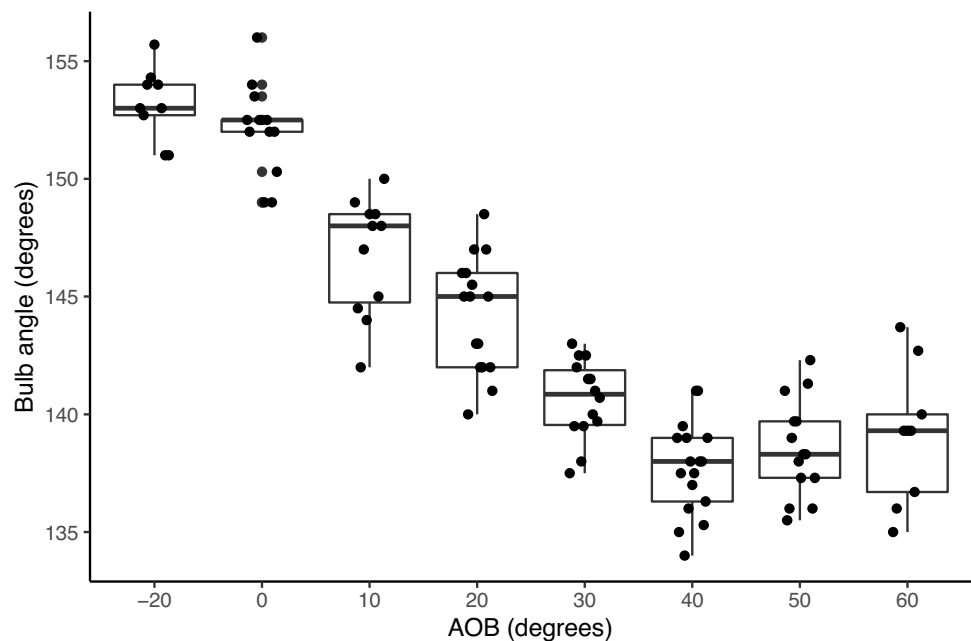
Fig. 7 Dotplot with error bar that indicates one standard deviation summarizing the relationship between bulb angle and angle of blow for flakes in the Dibble dataset (measured with the 1-mm intersection circle). Flakes measured with the vector calculation method are colored in gray. Flakes measured with the virtual goniometer method are colored in yellow. The black dot represents the mean bulb angle
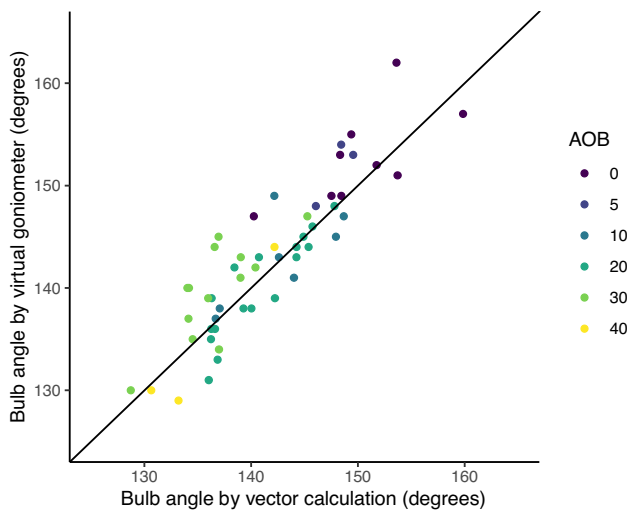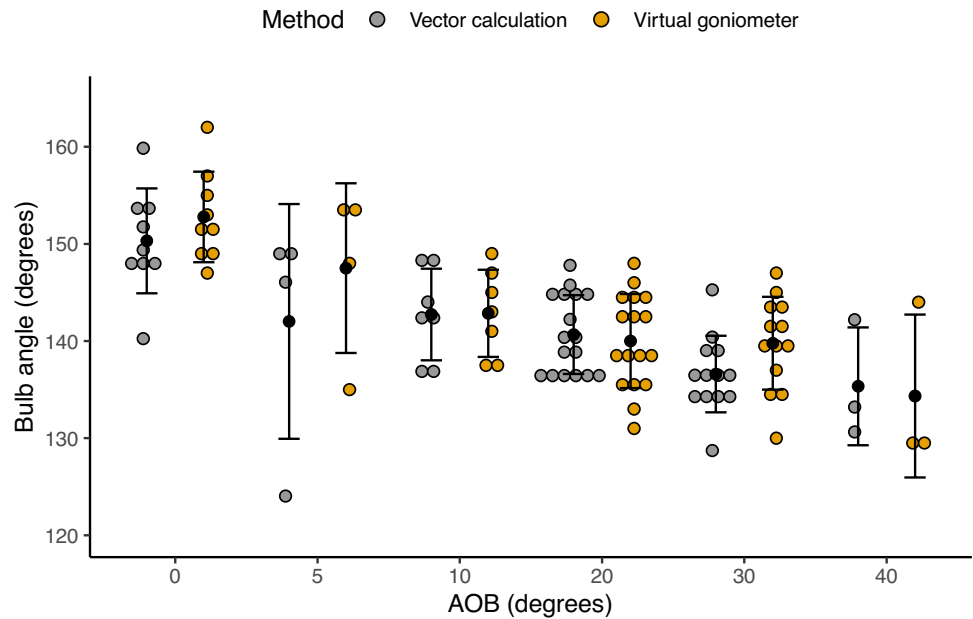

Fig. 8 Comparison of the flake bulb angles in the Dibble dataset as measured by the vector calculation method and by the virtual goniometer method (measured with the 1-mm intersection circle). The line represents a 1:1 correspondence

calculation bulb angle model, the overall regression was statistically significant ($R^2 = 0.50$, $F (3, 49) = 16.31$, $p < 0.001$). Both the angle of blow ($p < 0.001$) and platform depth ($p = 0.01$) were shown to significantly predict bulb angle. However, these two variables are correlated in the Dibble dataset. For the virtual goniometer bulb angle model, the overall regression was statistically significant ($R^2 = 0.48$, $F (3, 49) = 15.24$, $p < 0.001$). Only the angle of blow was shown to significantly predict bulb angle ($p < 0.001$). There was also a significant correlation between the angle of

blow and platform depth (*adj. $R^2 = 0.19$, $F (1, 51) = 13.59$, $p < 0.001$*).

MPI dataset

For the MPI dataset, the average standard error of the bulb angle is 0.7 degrees (see also Fig. 4.3 in SI 1). Figure 9 shows the distribution of bulb angle measured in this dataset. The average bulb angle for flakes is 132 degrees made with a high angle of blow and is 135.7 degrees for flakes made with a low angle of blow (see also Table 5.4 in SI 1). There is a significant difference in bulb angle between the knapper-assigned high and low angle of blow groups (Fig. 10, Kruskal–Wallis test, *$H = 9.11$, $p < 0.01$*).

Linear modeling

Using flakes from the Dibble dataset, Fig. 11a compares the actual flake mass to those predicted by the baseline EPA-PD model (Table 1). While the baseline model performs relatively well ($R^2 = 0.59$), it is clear that the flakes made with a lower angle of blow tend to have their mass underestimated, and the flakes made with a higher angle of blow tend to have their mass overestimated by the EPA-PD model. In comparison, when the known angle of blow is included as a predictor in addition to EPA and PD, the explanatory power of the model increased considerably ($R^2 = 0.81$), predicted flake masses are much closer to their actual values, and the over- and underestimation by the angle of blow are no longer present (Fig. 11b). An ANOVA test shows that the addition of angle of blow to the EPA-PD model significantly

Fig. 9 Histogram showing the distribution of bulb angle with overlaying density curve for all flakes analyzed in the MPI dataset
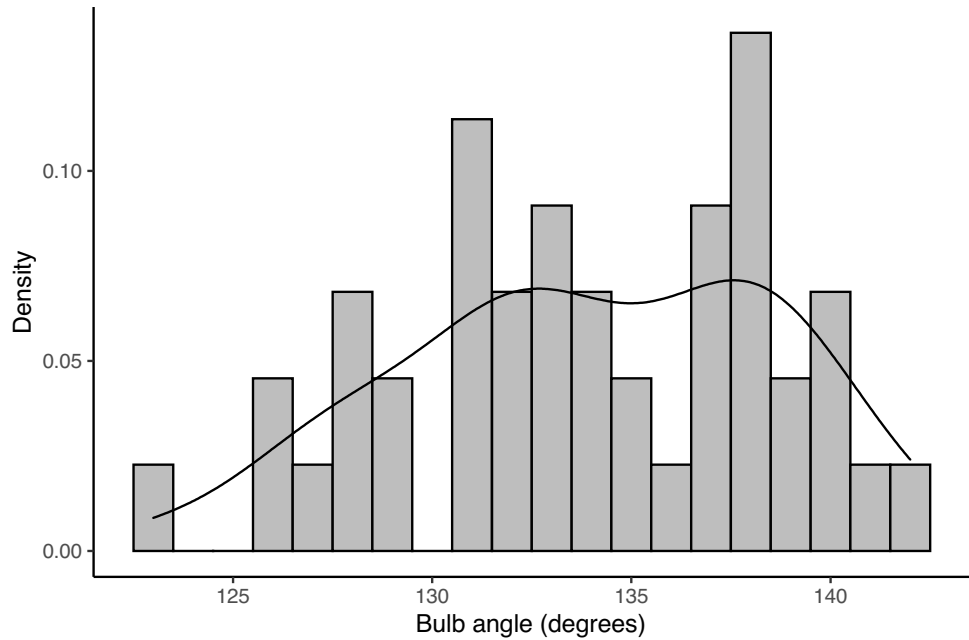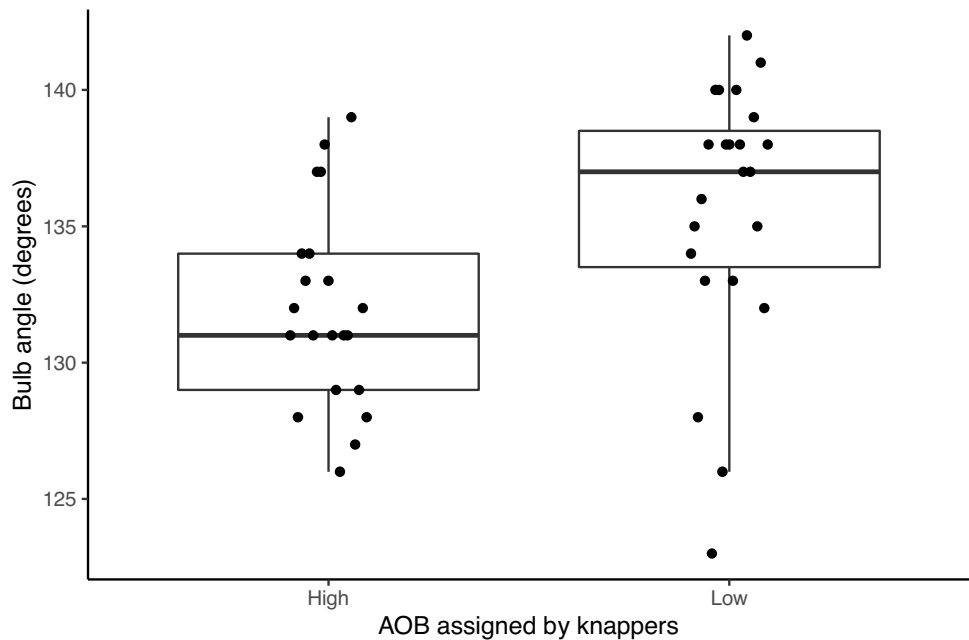

Fig. 10 Boxplot showing the result of the angle of blow blind test with the MPI dataset

improves the model's performance ($p < 0.001$, see also 6.4 in SI).

Figure 11c and d show the relationship between the actual versus the predicted flake mass based on the EPA-PD model and the inclusion of the bulb angles measured by the two methods with the 1-mm intersection circle. While the improvement in R^2 is not as strong as what we observed earlier with the use of the actual angles of blow values, the addition of the bulb angles still substantially increased the explanatory power of the linear model (Table 1). This observation is reflected by the ANOVA tests showing that adding the bulb angle (measured with both the vector calculation and the virtual goniometer methods) as a predictor of EPA and PD does significantly increase the amount of flake mass variation accountable by the linear model ($p < 0.001$, see also 6.4 in SI).

Discussion

Reconstructing knapping gestures from the archeological record is an important pathway to understanding the early knappers' tool use behavior. Up to now, the angle of blow

Fig. 11 Comparison of the actual flake mass and modeled flake mass in the Dibble dataset with a 95% confidence interval, $n = 53$. (a) Actual to predicted flake mass using the basic EPA-PD model, (b) actual to predicted flake mass using the EPA-PD-AOB model, (c) actual to predicted flake mass using the EPA-PD-BA (vector calculation) model, and (d) actual to predicted flake mass using the EPA-PD-BA (virtual goniometer) model
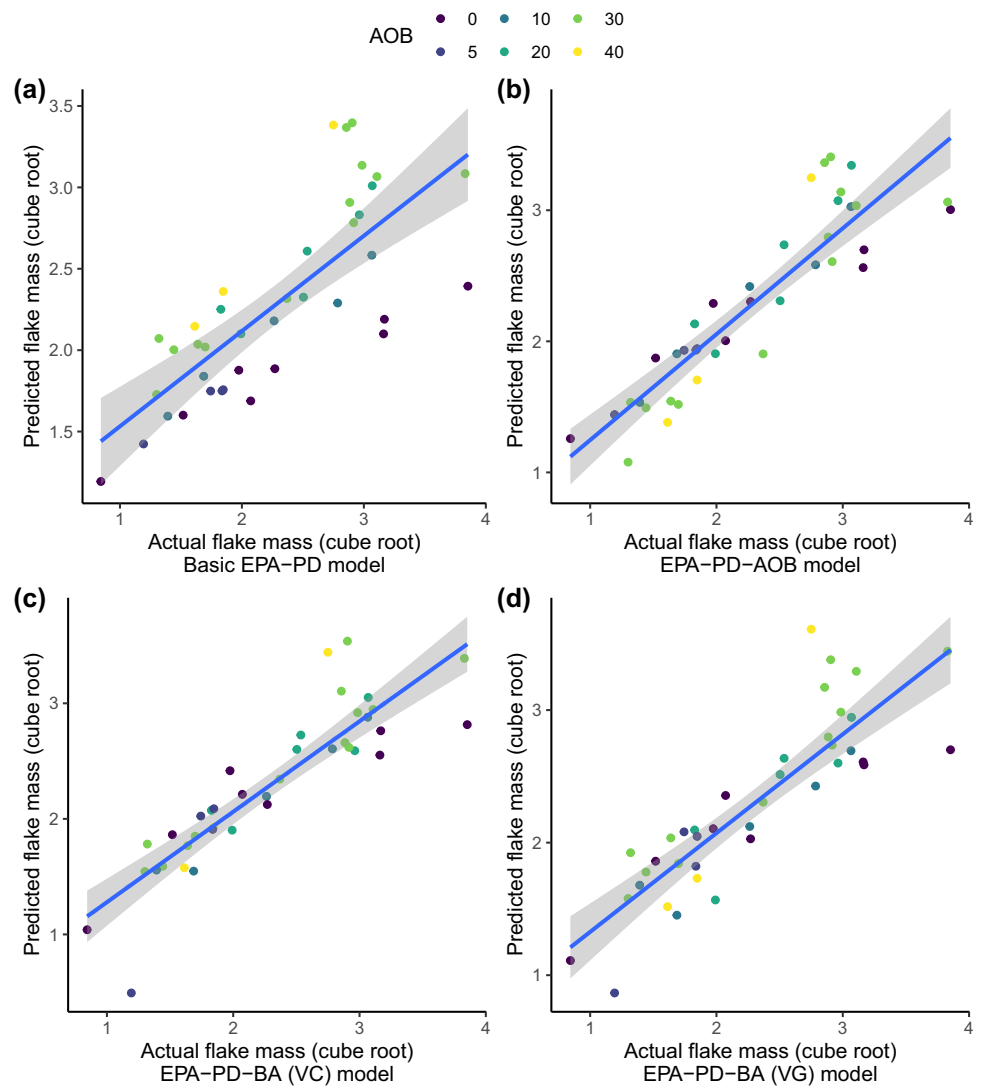

Table 1 Summary statistics of the different EPA-PD models

	Basic EPA-PD model	EPA-PD-AOB model	EPA-PD-BA (VC) model	EPA-PD-BA (VG) model
R^2	0.59	0.81	0.78	0.75
Adj. R^2	0.56	0.79	0.76	0.72
F statistics	25.41(2,36)	49(3,35)	42.04(3,35)	34.17(3,35)
p value	*<0.001*	*<0.001*	*<0.001*	*<0.001*

has been considered to be archeologically invisible (Magnani et al. 2014). In this study, we hypothesized that the angle of blow can in fact be gauged by the immediate angle between the striking platform and the protruding side of the Hertzian cone, what we referred to as the bulb angle. The results across all three datasets examined here support the hypothesis by showing that the bulb angle does indeed correlate with the angle of blow. Increasing the angle of blow during flake removal (i.e., greater tilt) causes the bulb angle to decrease, while a lower angle of blow (i.e., more

direct) results in higher bulb angle values. Importantly, this relationship is consistent among flakes made from different raw materials (soda-lime glass and flint) and under both mechanical and flintknapping experiments, suggesting that the correlation between the bulb angle and the angle of blow can be generalized to other flake formation settings.

The relationship between the bulb angle and the angle of blow is warranted by the fracture mechanics of Hertzian cone formation (Zeng et al. 1992; Kocer and Collins 1998; Gorham and Salman 2005; Marimuthu et al. 2016). Despite

its close relevance to flake formation, the field of fracture mechanics has had relatively little impact on lithic studies, likely owing to its mathematically laden nature and possibly to diverging goals. As previously discussed, earlier fracture mechanics-based controlled lithic experiments in the 1970s and 1980s emphasized testing ideas that directly come from the fracture mechanics literature. Unfortunately, results from these studies were not well applied to the actual archeological record (Speth 1972; Cotterell et al. 1985; Cotterell and Kamminga 1987). Although several studies have incorporated the orientation of the Hertzian cone to infer handedness of the knappers (Rugg and Mullane 2001; Bargalló and Mosquera 2014; Dominguez-Ballesteros and Arrizabalaga 2015), they did not establish a direct link between features of the Hertzian cone and the relevant knapping gestures. Instead, more recent controlled experiments have largely focused on assessing the empirical effects on flaking outcomes from knapping parameters that are under the direct control of knappers (Dibble and Whittaker 1981; Dibble and Pelcin 1995; Pelcin 1996; Dibble and Rezek 2009; Rezek et al. 2011; Magnani et al. 2014; Leader et al. 2017; Mraz et al. 2019; Dogandžić et al. 2020). This knapper-guided approach aims to establish statistical relationships between independent factors (e.g., EPA and PD) and dependent flake attributes, which can then be applied to infer past technological patterns from archeological finds (Davis and Shea 1998; Shott et al. 2000; Clarkson and Hiscock 2011; Muller and Clarkson 2014, 2016).

Here we expand on this knapper-guided approach by taking previous observations about the effect of the angle of blow and then incorporating fracture mechanics theory to help develop and test a hypothesis about the relationship between the angle of blow and the bulb angle. Importantly, the fracture mechanics model of Hertzian cone formation allowed us to make simple yet explicit predictions about what the bulb angles should be under different angles of blow. To this end, the experimental results show a relatively good agreement with these predicted values. For example, in the drop tower dataset, the average bulb angle on soda-lime glass flakes made with a zero angle of blow is 152 degrees, which is close to our theoretical prediction of 158 degrees based on the empirical value of the Hertzian cone angle for soda-line glass.

Compared to the drop tower dataset, the bulb angle values among the Dibble dataset associated with a zero angle of blow are a little lower (148.4 and 150.3 degrees) when measured with the 1-mm intersection circle radius. The bulb angle values, however, are significantly lower across all angles of blow groups when measured with larger intersection circle radii of 2 mm and 3 mm (Table 5.3 in SI 1). This is likely because the larger intersection circle radii capture the curvature beyond the original Hertzian cone crack when measuring bulb angle. The resulting bulb angle is

thereby not an accurate representation of the angle between the Hertzian cone crack and the platform surface, leading to the rather big discrepancy as we observe in the Dibble dataset. The use of the 3D models for the Dibble dataset also involved additional sources of error associated with the scanning and model processing procedure. In particular, the area of the flake at which the bulb angle was measured has a relatively complex morphology, such that minor variation in scan quality and levels of smoothing may substantially influence the measurements taken. Future studies should evaluate the influence of scan quality on the accuracy and precision of the bulb angle measurement. In the remaining discussion of results from the Dibble dataset, we will use the bulb angle values measured with the 1-mm intersection circle, which more accurately reflect the effect of the angle of blow on the orientation of the Hertzian cone.

For the drop tower dataset, the bulb angle stabilized at around 138 degrees once the angle of blow reached 40 degrees and beyond. This angle is close to the constant Hertzian cone angle of 136 degrees in soda-lime glass. As we outlined earlier in Fig. 1b, this minimum bulb angle likely represents the maximum tilt that the Hertzian cone can achieve when one side of the cone comes up against the platform surface. When the angle of blow reaches past 40 degrees, the Hertzian cone cannot tilt up any farther, and the bulb angle becomes plateaued at a value that is close to the Hertzian cone angle constant. However, we were not able to verify this hypothesis further with the Dibble dataset, as the sample size of the flakes in the Dibble dataset made with an angle of blow larger than 40 degrees is too small to allow meaningful statistical comparison. Future studies should thus investigate whether there is a similar threshold in the angle of blow at which point the bulb angle stabilizes under different knapping conditions and raw materials. There are also other differences between the Dibble dataset and the drop tower experiment that may influence the Hertzian cone formation. While most fracture mechanics studies that investigate Hertzian cone formation are conducted with spherical indenters (Frank and Lawn 1967; Chaudhri and Chen 1989; Fischer-Cripps 2007; Marimuthu et al. 2016), a flat-bevel ended hammer was used in the experiments that created the Dibble dataset. The non-spherical hammer tip may cause additional complications in the Hertzian cone formation (Fischer-Cripps 2007).

For both the drop tower dataset and Dibble dataset, the bulb angle linear models show that the angle of blow is the only variable that could significantly predict bulb angle, for the most part. The only exception is that in the Dibble dataset, platform depth appears to also influence bulb angle (when measured using the vector calculation method) in addition to the angle of blow. However, it should be noted that there is a significant correlation between the angle of blow and platform depth in the Dibble dataset because of

the way the experiments were structured in the first place (i.e., not all angles of blow were attempted for all platform depths). For this reason, platform depth also correlates with bulb angle, and there is no reason to think that platform depth influences bulb angle.

Though the results of the blind test on the MPI data show that bulb angles on high and low angles of blow flakes differ from each other on average, it is clear that relaxing the controls of the previous experiments makes the differences less apparent. One point of caution concerns the use of hammerstones in the experiment. These were not strictly controlled between strikes. While the size of the hammer does not change the Hertzian cone angle for a particular raw material type, it may influence how the cone responds to changes in the strike angle. Similarly, changes in the platform surface morphology may also alter the intended angle of blow. We also think it is likely that despite their intention to use specifically either a low or high angle of blow, the knappers might differ in their consistency as they rotated the core or adjusted their swing such that the angle changed in the opposite direction of their intention. It is possible, for instance, that while the arrangement of the core and overall arm movement should have led to a high angle of blow, for instance, small adjustments in the wrist orientation at strike may have lowered the angle.

It is important to emphasize here that the Hertzian cone angle varies by raw material. Specifically, it seems that the Hertzian cone angle is related to the mechanical properties of the material, such as the Poisson's ratio (Frank and Lawn, 1967; Kocer and Collins, 1998; Roesler, 1956). Raw materials with a larger Poisson's ratio, or those that are stiffer, have a larger cone angle (Olivi-Tran et al. 2020). As a result, we expect that the bulb angle produced when striking a core with a zero angle of blow will vary by raw material type. A larger Hertzian cone angle will result in a larger bulb angle for any given angle of blow. Similarly, the point at which the bulb angle plateaus with the angle of blow will vary as well. In fact, raw materials with larger Hertzian cone angles should plateau sooner, and the range of angles of blow that can be measured on these materials will be more limited. On the contrary, raw materials with smaller Hertzian cone angles will allow a greater range of angles of blow to be measured. This potential discrepancy in the range of bulb angle variation in different raw materials could further complicate our interpretation of actual archeological assemblages where raw material types vary. For now, until the Hertzian cone angle is known for the appropriate raw material types, comparisons in bulb angles are best done within a given raw material type. Drawing on information from the available fracture mechanics studies, it is also possible to estimate the range of variation of the Hertzian cone angle for a raw material with known mechanical properties such as Poisson's ratio (Chaudhri 2015; Olivi-Tran et al. 2020).

The linear model results show that the angle of blow is an important knapping parameter that can help improve our ability to explain flake variation using independent flake variables, such as exterior platform angle and platform depth. The current EPA-PD model of flake formation derived from the controlled experiments by Dibble and colleagues only addresses a portion of the variation in flake size and shape (Dibble and Rezek 2009; Rezek et al. 2011; Magnani et al. 2014; Leader et al. 2017; Dogandžić et al. 2020; McPherron et al. 2020). The EPA-PD model often performs less well when applied to less controlled experimental replication assemblages and archeological assemblages. Although several studies have attempted to improve the EPA-PD model by adding other attributes such as platform width, platform area, and platform shape (Dibble 1997; Davis and Shea 1998; Shott et al. 2000; Clarkson and Hiscock 2011; Lin et al. 2013; Dogandžić et al. 2015; Shott and Seeman 2017; Režek et al. 2018; McPherron et al. 2020), the ability of the model and its variants to accurately predict the original flake size is still limited. In their paper on the topic, Dibble and Rezek (2009) found that exterior platform angle, platform depth, and angle of blow all influenced flake mass, yet the angle of blow was mostly dropped from subsequent presentations of the model because the parameter could not be measured on the flakes themselves (see also Shott and Seeman 2017). Our results show that the inclusion of the angle of blow into the EPA-PD model significantly improved the model performance. More importantly, we further showed that substituting bulb angle for angle of blow resulted in a similar improvement in model's R^2, indicating that the bulb angle is a useful proxy for gauging the angle of blow used to make flakes.

Here we have been looking at the effect of exterior platform angle, platform depth, and the angle of blow on flake mass as a measure of how well our model of how flakes form and how they vary is working. However, the EPA-PD model's key feature of predicting the original blank size can facilitate the analysis of stone tool reduction by quantifying mass loss in addition to traditional methods such as studying the morphological features, scar density, and cortex ratio of stone tools (Dibble 1987; Rolland and Dibble 1990; Kuhn 1990; Braun et al. 2008; Shipton and Clarkson 2015). As discussed in many studies, an accurate measurement of the degree of reduction is crucial for studying the curation and use life of stone tools (Binford 1973; Shott 1996; Shott et al. 2000; Clarkson and Hiscock 2011). By offering an improved estimation of the original blank size, the EPA-PD-BA model contributes to the study of stone tool curation and use life, which also provides insight into understanding hominin mobility and site occupation.

Conclusions

Our findings, for the first time, demonstrate a quantitative method for measuring the angle at which knappers strike the hammer during flake removal, or the angle of blow, from a measurable flake attribute—the bulb angle. While both researchers and modern knappers have long noted the significance of this parameter in successful flake removal and in learning skill of knapping, up to now the variable has been largely considered to be invisible in the archeological record. The ability to gauge the angle of blow among archeological flakes by using the bulb angle opens a range of new research opportunities to study how hominins managed this important component of force delivery in knapping stone flakes over the past 2–3 million years. Importantly, given that the angle of blow has been repeatedly shown to be an important factor in the learning of stone working among modern knappers, quantifying changes in the angle of blow among Paleolithic flake assemblages may offer new insights into the evolution of human technology and cultural transmission.

It is important to keep in mind that the bulb angle measurement may be complicated by other sources of variation. Not only is the bulb angle a small-sized feature that can be prone to measurement error, but factors such as raw material, hammer size and shape, and the initial nodule condition may also all contribute to variation in the bulb angle. As with any newly developed methods, we urge for more studies to test the reliability of the bulb angle, especially under more diverse experimental settings. Lastly, our study shows that incorporating fracture mechanics provides promising insights and inspirations to translate different knapping behaviors to tangible flake attributes (McPherron et al. 2020). To this end, exploring force delivery variables such as striking force and hammer size and velocity from a fundamental perspective of flaking mechanics can be a fruitful avenue forward, helping to establish connections between quantitative flake attributes with the dynamic manual gesture and knapping techniques of past hominins.

Declarations

References

Archer W, Pop CM, Rezek Z et al (2018) A geometric morphometric relationship predicts stone flake shape and size variability. Archaeol Anthropol Sci 10:1991–2003

Baena J, Moncel M-H, Cuartero F et al (2017) Late Middle Pleistocene genesis of Neanderthal technology in Western Europe: the case of Payre site (south-east France). Quatern Int 436:212–238

Bargalló A, Mosquera M (2014) Can hand laterality be identified through lithic technology? Laterality: asymmetries of body, brain and cognition 19:37–63

Bataille G, Conard NJ (2018) Blade and bladelet production at Hohle Fels Cave, AH IV in the Swabian Jura and its importance for characterizing the technological variability of the Aurignacian in Central Europe. PLoS ONE 13:e0194097

Binford LR (1973) Interassemblage variability: the Mousterian and the 'functional' argument. The Explanation of Culture Change: Models in Prehistory, edited by C Renfrew 227–254

Biryukova EV, Bril B (2008) Organization of goal-directed action at a high level of motor skill: the case of stone knapping in India. Mot Control 12:181–209

Boëda E (1995) Levallois: a volumetric construction, methods, a technique. In: The definition and interpretation of Levallois technology. Prehistory Press Madison, pp 41–65

Braun DR, Tactikos JC, Ferraro JV et al (2008) Oldowan reduction sequences: methodological considerations. J Archaeol Sci 35:2153–2163

Braun DR, Aldeias V, Archer W et al (2019) Earliest known Oldowan artifacts at> 2.58 Ma from Ledi-Geraru, Ethiopia, highlight early technological diversity. Proc Natl Acad Sci 116:11712–11717

Bril B, Rein R, Nonaka T et al (2010) The role of expertise in tool use: skill differences in functional action adaptations to task constraints. J Exp Psychol Hum Percept Perform 36:825–839

Chaudhri MM (2015) Dynamic fracture of inorganic glasses by hard spherical and conical projectiles. Philo Trans Royal Soc a: Math, Phys Eng Sci 373:20140135

Chaudhri MM, Chen L (1989) The orientation of the Hertzian cone crack in soda-lime glass formed by oblique dynamic and quasi-static loading with a hard sphere. J Mater Sci 24:3441–3448

Cignoni P, Callieri M, Corsini M, et al (2008) Meshlab: an open-source mesh processing tool. In: Eurographics Italian chapter conference. Salerno, Italy, pp 129–136

Clarkson C, Hiscock P (2011) Estimating original flake mass from 3D scans of platform area. J Archaeol Sci 38:1062–1068

Cotterell B, Kamminga J (1987) The formation of flakes. Am Antiq 52:675–708. https://doi.org/10.2307/281378

Cotterell B, Kamminga J, Dickson FP (1985) The essential mechanics of conchoidal flaking. Int J Fract 29:205–221. https://doi.org/10.1007/BF00125471

Crabtree DE (1972) The cone fracture principle and the manufacture of lithic materials. Tebiwa 15:29–42

Cueva-Temprana A, Lombao D, Morales JI et al (2019) Gestures during knapping: a two-perspective approach to Pleistocene Technologies. Lithic Technol 44:74–89

Davis ZJ, Shea JJ (1998) Quantifying lithic curation: an experimental test of Dibble and Pelcin's original flake-tool mass predictor. J Archaeol Sci 25:603–610

Delagnes A, Roche H (2005) Late Pliocene hominid knapping skills: the case of Lokalalei 2C, West Turkana, Kenya. J Hum Evol 48:435–472

Dibble HL (1987) Reduction sequences in the manufacture of Mousterian implements of France. In: The Pleistocene Old World. Springer, pp 33–45

Dibble HL (1997) Platform variability and flake morphology: a comparison of experimental and archaeological data and implications for interpreting prehistoric lithic technological strategies. Lithic Technol 22:150–170

Dibble HL, Pelcin A (1995) The effect of hammer mass and velocity on flake mass. J Archaeol Sci 22:429–439

Dibble HL, Rezek Z (2009) Introducing a new experimental design for controlled studies of flake formation: results for exterior platform angle, platform depth, angle of blow, velocity, and force. J Archaeol Sci 36:1945–1954

Dibble HL, Whittaker JC (1981) New experimental evidence on the relation between percussion flaking and flake variation. J Archaeol Sci 8:283–296

Dogandžić T, Braun DR, McPherron SP (2015) Edge length and surface area of a blank: experimental assessment of measures, size predictions and utility. PLoS ONE 10:e0133984

Dogandžić T, Abdolazadeh A, Leader G et al (2020) The results of lithic experiments performed on glass cores are applicable to other raw materials. Archaeol Anthropol Sci 12:44

Dominguez-Ballesteros E, Arrizabalaga A (2015) Flint knapping and determination of human handedness. Methodological proposal with quantifiable results. J Archaeol Sci Rep 3:313–320

Eren MI, Lycett SJ, Patten RJ et al (2016) Test, model, and method validation: the role of experimental stone artifact replication in hypothesis-driven archaeology. Ethnoarchaeology 8:103–136

Fischer-Cripps AC (2007) Introduction to contact mechanics. Springer, New York

Forestier H (1992) Approche technologique de quelques séries dites clactoniennes du nord-ouest de la France et du sud-est de l'Angleterre. Université Paris X Nanterre, Mémoire de Maîtrise

Frank FC, Lawn B (1967) On the theory of Hertzian fracture. Proc R Soc Lond A 299:291–306

Geribàs N, Mosquera M, Vergès JM (2010) The gesture substratum of stone tool making: an experimental approach. Sezione Di Museologia Scientifica e Naturalistica 6:155–162

Gorham DA, Salman AD (2005) The failure of spherical particles under impact. Wear 258:580–587

Hellweg P (1984) Flintknapping: the art of making stone tools. Canyon Publishing Company

Key A, Fisch MR, Eren MI (2018) Early stage blunting causes rapid reductions in stone tool performance. J Archaeol Sci 91:1–11

Kocer C, Collins RE (1998) Angle of Hertzian cone cracks. J Am Ceram Soc 81:1736–1742

Kuhn SL (1990) A geometric index of reduction for unifacial stone tools. J Archaeol Sci 17:583–593. https://doi.org/10.1016/0305-4403(90)90038-7

Lawn BR, Wilshaw TR, Hartley NEW (1974) A computer simulation study of Hertzian cone crack growth. Int J Fract 10:1–16

Lawn BR, Wiederhorn SM, Roberts DE (1984) Effect of sliding friction forces on the strength of brittle materials. J Mater Sci 19:2561–2569

Leader G, Abdolahzadeh A, Lin SC, Dibble HL (2017) The effects of platform beveling on flake variation. J Archaeol Sci Rep 16:213–223

Lin SC, Rezek Z, Braun D, Dibble HL (2013) On the utility and economization of unretouched flakes: the effects of exterior platform angle and platform depth. Am Antiq 78:724–745

Lycett SJ (2013) Cultural transmission theory and fossil hominin behaviour. Understanding Cultural Transmission in Anthropol: a Critical Synthesis 26:102

Lycett SJ, von Cramon-Taubadel N, Eren MI (2016) Levallois: potential implications for learning and cultural transmission capacities. Lithic Technol 41:19–38

Macchi R, Daver G, Brenet M et al (2021) Biomechanical demands of percussive techniques in the context of early stone toolmaking. J R Soc Interface 18:20201044

Magnani M, Rezek Z, Lin SC et al (2014) Flake variation in relation to the application of force. J Archaeol Sci 46:37–49

Marimuthu KP, Rickhey F, Lee H, Lee JH (2016) Spherical indentation cracking in brittle materials: an XFEM study. In: 2016 7th International Conference on Mechanical and Aerospace Engineering (ICMAE). IEEE, pp 267–273

Marzke MW (2013) Tool making, hand morphology and fossil hominins. Philo Trans Royal Soc b: Biol Sci 368:20120414

McPherron SP, Abdolahzadeh A, Archer W, et al (2020) Introducing platform surface interior angle (PSIA) and its role in flake formation, size and shape. Manuscript submitted for publication

Morgan TJ, Uomini NT, Rendell LE et al (2015) Experimental evidence for the co-evolution of hominin tool-making teaching and language. Nat Commun 6:1–8

Mraz V, Fisch M, Eren MI et al (2019) Thermal engineering of stone increased prehistoric toolmaking skill. Sci Rep 9:1–8. https://doi.org/10.1038/s41598-019-51139-3

Muller A, Clarkson C (2014) Estimating original flake mass on blades using 3D platform area: problems and prospects. J Archaeol Sci 52:31–38

Muller A, Clarkson C (2016) Identifying major transitions in the evolution of lithic cutting edge production rates. PLoS ONE 11:e0167244

Nonaka T, Bril B, Rein R (2010) How do stone knappers predict and control the outcome of flaking? Implications for understanding early stone tool technology. J Hum Evol 59:155–167. https://doi.org/10.1016/j.jhevol.2010.04.006

Olivi-Tran N, Despetis F, Faivre A (2020) Modeling of deep indentation in brittle materials. Mater Res Express 7:035201

Pargeter J, Khreisheh N, Stout D (2019) Understanding stone tool-making skill acquisition: experimental methods and evolutionary implications. J Hum Evol 133:146–166

Pelcin AW (1996) Controlled experiments in the production of flake attributes

Pelegrin J (1993) A framework for analysing prehistoric stone tool manufacture and a tentative application to some early stone industries. The use of tools by human and non-human primates 30214:

R Core Team (2020) R: a language and environment for statistical computing. R Foundation for Statistical Computing, Vienna, Austria

Rein R, Bril B, Nonaka T (2013) Coordination strategies used in stone knapping. Am J Phys Anthropol 150:539–550

Rezek Z, Lin S, Iovita R, Dibble HL (2011) The relative effects of core surface morphology on flake shape and other attributes. J Archaeol Sci 38:1346–1359

Režek Ž, Dibble HL, McPherron SP et al (2018) Two million years of flaking stone and the evolutionary efficiency of stone tool technology. Nature Ecol & Evol 2:628

Roche H, Delagnes A, Brugal J-P et al (1999) Early hominid stone tool production and technical skill 2.34 Myr ago in West Turkana. Kenya Nature 399:57–60. https://doi.org/10.1038/19959

Roesler FC (1956) Brittle fractures near equilibrium. Proc Phys Soc London, Sect B 69:981

Rolian C, Lieberman DE, Zermeno JP (2011) Hand biomechanics during simulated stone tool use. J Hum Evol 61:26–41

Rolland N, Dibble HL (1990) A new synthesis of Middle Paleolithic variability. Am Antiq 55:480–499

Roussel M, Bourguignon L, Soressi M (2009) Identification par l'expérimentation de la percussion au percuteur de calcaire au Paléolithique moyen: le cas du façonnage des racloirs bifaciaux Quina de Chez Pinaud (Jonzac, Charente-Maritime). Bulletin de la Société préhistorique française 219–238

Rugg G, Mullane M (2001) Inferring handedness from lithic evidence. Laterality: asymmetries of Body. Brain Cogn 6:247–259

Salman AD, Gorham DA, Verba A (1995) A study of solid particle failure under normal and oblique impact. Wear 186:92–98

Schmid VC, Porraz G, Zeidi M, Conard NJ (2019) Blade technology characterizing the MIS 5 DA layers of Sibudu Cave, South Africa. Lithic Technol 44:199–236

Schmid VC, Douze K, Tribolo C, et al (2021) Middle Stone Age Bifacial Technology and Pressure Flaking at the MIS 3 Site of Toumboura III, Eastern Senegal. African Archaeological Review 1–33

Shipton C (2018) Biface knapping skill in the East African Acheulean: progressive trends and random walks. Afr Archaeol Rev 35:107–131

Shipton C, Clarkson C (2015) Handaxe reduction and its influence on shape: an experimental test and archaeological case study. J Archaeol Sci Rep 3:408–419

Shott MJ (1996) An exegesis of the curation concept. J Anthropol Res 52:259–280

Shott MJ, Seeman MF (2017) Use and multifactorial reconciliation of uniface reduction measures: a pilot study at the Nobles Pond Paleoindian site. Am Antiq 82:723–741

Shott MJ, Bradbury AP, Carr PJ, Odell GH (2000) Flake size from platform attributes: predictive and empirical approaches. J Archaeol Sci 27:877–894

Snyder WD, Reeves JS, Tennie C (in press) Early knapping techniques do not necessitate cultural transmission. Science Advances

Soriano S, Villa P, Wadley L (2007) Blade technology and tool forms in the Middle Stone Age of South Africa: the Howiesons Poort and post-Howiesons Poort at rose Cottage Cave. J Archaeol Sci 34:681–703

Speth JD (1972) Mechanical basis of percussion flaking. Am Antiq 37:34–60. https://doi.org/10.2307/278884

Speth JD (1975) Miscellaneous studies in hard-hammer percussion flaking: the effects of oblique impact. American Antiquity 203–207

Suh C-M, Kim D-K, Lee M-H (2006) A study on damage behavior of glass by oblique impact of steel ball. Int J Mod Phys B 20:4291–4296

Susman RL (1998) Hand function and tool behavior in early hominids. J Hum Evol 35:23–46

Tennie C, Braun DR, Premo LS, McPherron SP (2016) The Island test for cumulative culture in the Paleolithic. In: The nature of culture. Springer, pp 121–133

Tennie C, Premo LS, Braun DR, McPherron SP (2017) Early stone tools and cultural transmission: resetting the null hypothesis. Current anthropology: a world journal of the sciences of man 652–672

Texier PJ, Roche H (1995) The impact of predetermination on the development of some Acheulean chaînes opératoires. Evolución Humana En Europa y Los Yacimientos De La Sierra De Atapuerca 2:403–420

Valletta F, Smilansky U, Goring-Morris AN, Grosman L (2020) On measuring the mean edge angle of lithic tools based on 3-D models–a case study from the southern Levantine Epipalaeolithic. Archaeol Anthropol Sci 12:1–19

Van Rossum G, Drake FL (2011) The python language reference manual. Network Theory Ltd.

Vernooij CA, Mouton LJ, Bongers RM (2015) Learning to control orientation and force in a hammering task. Zeitschrift für Psychologie

Waldorf DC (2006) The art of flint knapping, 5th edn. Mound Builder Books

Whittaker JC (1994) Flintknapping: making and understanding stone tools. University of Texas Press

Williams EM, Gordon AD, Richmond BG (2012) Hand pressure distribution during Oldowan stone tool production. J Hum Evol 62:520–532

Yezzi-Woodley K, Calder J, Olver PJ et al (2021) The virtual goniometer: demonstrating a new method for measuring angles on archaeological materials using fragmentary bone. Archaeol Anthropol Sci 13:1–16

Zeng K, Breder K, Rowcliffe DJ (1992) The Hertzian stress field and formation of cone cracks—I. Theoretical Approach Acta Metallurgica Et Materialia 40:2595–2600